FINITE-OFFSET CRS: PARAMETRISATION AND ATTRIBUTE PREDICTION

C. Vanelle, S. Wißmath, and D. Gajewski

email: *claudia.vanelle@uni-hamburg.de*
keywords: *Offset CRS, traveltimes*

ABSTRACT

Multiparameter stacking methods provide the foundation for many applications in seismic imaging. One important example for such an application is prestack data enhancement by partial common reflection surface (CRS) stacking. Currently, this technique is based on parameters determined from zero-offset CRS processing, which limits the accuracy of reconstructed traces for far offsets. Although it is, in principle, possible to use parameters from the according finite-offset CRS, the determination of eight parameters in this case compared to three for zero offset is considerably more demanding. In this paper, we introduce a CRS parametrisation for the finite offset case that is not only more intuitive than a previously-introduced formulation, but it also allows to predict offset parameters from the zero-offset parameters. A generic example confirms the accuracy of the prediction, which is exact for planar reflectors.

INTRODUCTION

Multiparameter stacking methods serve as important tools in applied seismics. In addition to providing reliable time images of the subsurface, they lead to additional information in terms of stacking parameters, the so-called kinematic wavefield attributes. Over the past years, several operators have been introduced. They all aim to describe the traveltime moveout in both midpoint and offset direction for reflected and diffracted events with the highest possible accuracy. The most prominent operators are the shifted hyperbola (de Bazelaire, 1988), the common reflection surface (CRS, Müller, 1999), multifocusing (MF, Gelchinksy et al., 1999; Landa et al., 2010), and the recently-introduced i-CRS (Vanelle et al., 2010; Schwarz et al., 2014). In this work, we focus on the CRS method.

A clear physical interpretation of the CRS parameters exists for monotypic waves in the zero offset (ZO) case, where three parameters in two dimensions and eight in 3D describe the incidence/emergence angles and curvatures of two hypothetical wavefronts at the CMP under consideration. A physical interpretation for the finite offset (FO) case was introduced by Zhang et al. (2001, 2002).

The parameters are often determined with a 'pragmatic approach' (Jäger et al., 2001), where each parameter is initially obtained from a one-dimensional search procedure before a simultaneous optimisation is carried out, using the parameters from the individual 1D searches as starting values.

Since a multidimensional search is computationally expensive, such an efficient strategy becomes more important the higher the number of parameters is. This is particularly the case when the step from zero to finite offset is taken or wave type conversion occurs. Then, the number of parameters increases to five in 2D and fourteen in 3D.

The results of the CRS method are the wavefield attributes that are useful for a large variety of potential applications. In particular, the prestack data enhancement method by means of partial stacking introduced by Baykulov and Gajewski (2009) have recently gained importance as it provides not only prestack data with an improved signal-to-noise ratio but it is also a useful tool for data regularisation. So far, partial

CRS relies on the ZO attributes even if finite offsets are considered. The quality of the resulting enhanced prestack data would benefit from FO parameters, especially if larger offsets are considered.

Although a method for the prediction of FO-CRS parameters was recently suggested by Bauer et al. (2014b) and Bauer et al. (2014a), it is only applicable in the presence of diffractions. In this work, we introduce two steps toward a prediction of FO CRS attributes that are also valid for reflections. In the first, we express the FO-CRS operator in a parametrisation that applies results from Zhang et al. (2001) and Vanelle (2012). We arrive at similar results as Zhang et al. (2001), however, we follow a different derivation, which leads to an operator that provides more physical insight than the traveltime formulation by Zhang et al. (2002). Based on the hyperbolic traveltime equation introduced by Vanelle and Gajewski (2002), we then derive expressions for the FO-CRS parameters for arbitrary midpoints and offsets in terms of the ZO- or even FO-CRS parameters of a neighbouring CMP, thus allowing the extrapolation to another offset.

Following the derivation of our FO-CRS traveltime parametrisation and the extrapolation of the attributes, we investigate the applicability of the method. The expressions are exact for plane reflectors with arbitrary inclination. Numerical studies in a simple model show that the method works well for curved reflectors, too. Although the predicted parameters may not be as highly accurate for more complex models, they can nevertheless provide starting values for the simultaneous optimisation and, therefore, improve the efficiency of the search algorithm. Furthermore, the parameter determination can be carried out in an iterative fashion.

METHOD

In this section, we introduce a FO-CRS traveltime expression with physically intuitive parametrisation and suggest how the parameters can be estimated from ZO- or FO-CRS parameters of a neighbouring CMP. For simplicity, we consider the 2D case in the derivation: while the derivation of the results for the corresponding 3D situation is straightforward (based on, e.g., Vanelle and Gajewski, 2002), it is also tedious and does not lead to new insights.

The general moveout equation

In source and receiver coordinates, the traveltime for an arbitrary source-receiver combination (s, g) in the vicinity of an expansion point at (s_0, g_0) can be expressed by the general moveout (GNMO) equation, the hyperbolic formula introduced by Vanelle and Gajewski (2002),

$$T^2(s,g) = (T_0 + q\,\Delta g - p\,\Delta s)^2 + T_0\,(G\,\Delta g^2 - S\,\Delta s^2 - 2\,N\,\Delta s\,\Delta g) \quad , \tag{1}$$

where Δs and Δg are the distances of the source and receiver positions, respectively, to the expansion point, i.e.

$$\Delta s = s - s_0 \quad \text{, and} \qquad \Delta g = g - g_0 \quad . \tag{2}$$

The traveltime T_0 is that in the expansion point, i.e., from s_0 to g_0. The coefficients in equation (1) are the first- and second-order derivatives of the traveltime with respect to source and receiver coordinates, namely the first-order derivatives,

$$p = -\left.\frac{\partial T}{\partial s}\right|_{s_0,g_0} \quad \text{, and} \qquad q = \left.\frac{\partial T}{\partial g}\right|_{s_0,g_0} \quad , \tag{3}$$

are the horizontal slownesses at the source and receiver, respectively. The second-order derivatives are given by

$$S = -\left.\frac{\partial^2 T}{\partial s^2}\right|_{s_0,g_0} \quad , \quad G = \left.\frac{\partial^2 T}{\partial g^2}\right|_{s_0,g_0} \quad \text{, and} \qquad N = -\left.\frac{\partial^2 T}{\partial s\,\partial g}\right|_{s_0,g_0} \quad . \tag{4}$$

In midpoint and half-offset coordinates (x_m, h), with

$$x_m = \frac{g+s}{2} \quad \text{, and} \qquad h = \frac{g-s}{2} \quad , \tag{5}$$

and using $\triangle h = h - h_0$, $\triangle x_m = x_m - x_0$, equation (1) becomes

$$\begin{aligned} T^2(x_m,h) &= \left(T_0 + (q-p)\,\triangle x_m + (q+p)\,\triangle h\right)^2 \\ &\quad + T_0\left((G-S-2\,N)\,\triangle x_m^2 + (G-S+2\,N)\,\triangle h^2 + 2\,(G+S)\,\triangle x_m\,\triangle h\right) \quad . \end{aligned} \tag{6}$$

This expression is the general moveout equation in midpoint and half-offset coordinates. We will now consider the zero-offset case and relate (6) to the ZO-CRS formulation.

Zero-offset: GNMO and CRS

In the zero-offset situation for monotypic waves, the traveltime expressions (1) and (6) must be symmetric with respect to interchanging the source and receiver, i.e., changing the sign of h. Therefore, the following relations apply:

$$q = -p \quad \text{and} \qquad G = -S \quad . \tag{7}$$

Furthermore, we have $h_0 = 0$ and, therefore, $\triangle h = h$. In conclusion, equation (6) reduces to

$$\begin{aligned} T^2(x_m,h) &= (T_0 + 2\,q\,\triangle x_m)^2 + 2\,T_0\left((G-N)\,\triangle x_m^2 + (G+N)\,h^2\right) \quad , \\ &= (T_0 - 2\,p\,\triangle x_m)^2 + 2\,T_0\left((-S-N)\,\triangle x_m^2 + (-S+N)\,h^2\right) \quad . \end{aligned} \tag{8}$$

We now consider the ZO-CRS formulation (e.g., Müller, 1999),

$$T^2(x_m,h) = (T_0 + 2\,\frac{\sin\alpha}{V_0}\,\triangle x_m)^2 + 2\,T_0\,\frac{\cos^2\alpha}{V_0}\left(K_N\,\triangle x_m^2 + K_{NIP}\,h^2\right) \quad , \tag{9}$$

where the angle α is the incidence angle against the normal to the registration line, and V_0 is the near-surface velocity. The curvatures K_N and K_{NIP} are the inverse of the radii R_N and R_{NIP} of the so-called N- and NIP-wavefronts (see Figure 1). Comparing the coefficients in equations (8) and (9), we find that the parameters of both expressions are related by

$$\begin{aligned} q = \frac{\sin\alpha}{V_0} &= -\,p \quad , \\ G = \frac{\cos^2\alpha}{2\,V_0}\,(K_{NIP} + K_N) &= -\,S \quad , \\ N = \frac{\cos^2\alpha}{2\,V_0}\,(K_{NIP} - K_N) \quad , & \end{aligned} \tag{10}$$

and accordingly,

$$\begin{aligned} K_N = \frac{V_0}{\cos^2\alpha}\,(G-N) &= \frac{V_0}{\cos^2\alpha}\,(-S-N) \quad , \\ K_{NIP} = \frac{V_0}{\cos^2\alpha}\,(G+N) &= \frac{V_0}{\cos^2\alpha}\,(-S+N) \quad , \\ \sin\alpha = q\,V_0 &= -p\,V_0 \quad . \end{aligned} \tag{11}$$

Finite-offset: GNMO and CRS

According to the zero-offset parameters in equation (11), we can formally express the common-offset parameters in terms of the derivatives in equation (1). These are, like in the ZO case, emergence and incidence angles as well as curvatures of fictitious wavefronts, which are generated at the reflection point and explained in Figure 2. As for the ZO case, they can be written as sums and differences of G, S, and N. In contrast to the ZO case, however, these waves are no longer normal to the interface, and neither does a

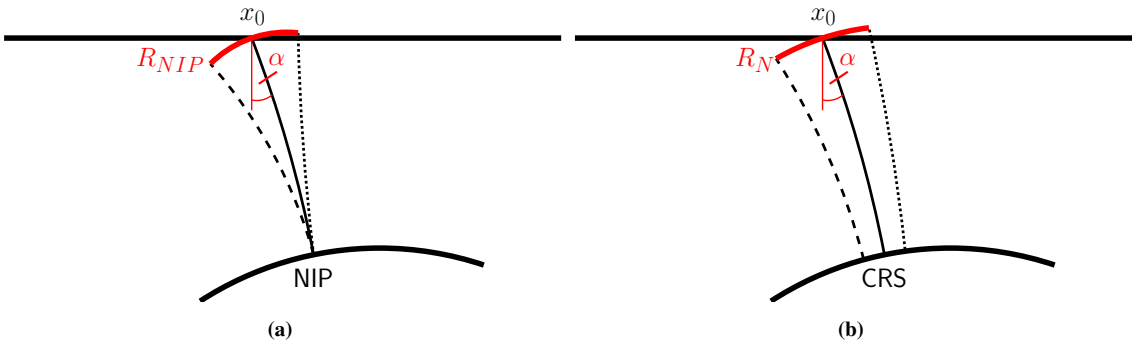

Figure 1: The meaning of the ZO-CRS parameters α, K_N and K_{NIP}: $K_{NIP} = 1/R_{NIP}$ is the curvature of a wavefront emitted by a fictitious point source at the normal incidence point (NIP), $K_N = 1/R_N$ is the wavefront curvature of the fictitious so-called normal wave that would be generated normal to the reflector by a region surrounding the normal incidence point, the common reflection surface (CRS), and α is the incidence angle. All parameters are considered at $s_0 = g_0 = x_0$ and $h = 0$.

normal incidence point exist. Therefore, we adopt the notation suggested by Zhang et al. (2002) and find the following expressions for the resulting FO parameters:

$$\begin{aligned} K^g_{CMP} &= \frac{v_g}{\cos^2\alpha_g}(G+N) \quad , \quad K^s_{CMP} = -\frac{v_s}{\cos^2\alpha_s}(-S+N) \quad , \\ K^g_{CO} &= \frac{v_g}{\cos^2\alpha_g}(G-N) \quad , \quad K^s_{CO} = -\frac{v_s}{\cos^2\alpha_s}(-S-N) \quad , \\ \sin\alpha_g &= q\,v_g \quad , \quad \sin\alpha_s = -p\,v_s \quad , \end{aligned} \tag{12}$$

and, respectively,

$$\begin{aligned} q &= \frac{\sin\alpha_g}{V_g} \quad , \quad p = \frac{\sin\alpha_s}{V_s} \quad , \\ G &= \frac{\cos^2\alpha_g}{2\,V_g}(K^g_{CMP}+K^g_{CO}) \quad , \quad S = \frac{\cos^2\alpha_s}{2\,V_s}(K^s_{CMP}+K^s_{CO}) \quad , \\ N &= \frac{\cos^2\alpha_g}{2\,V_g}(K^g_{CMP}-K^g_{CO}) \quad = \quad -\frac{\cos^2\alpha_s}{2\,V_s}(K^s_{CMP}-K^s_{CO}) \quad . \end{aligned} \tag{13}$$

The last equivalence follows from the fact that there are only five independent parameters.

The common-offset CRS formula by Zhang et al. (2001) uses the $K^{s,g}_{CMP}$ but not $K^{s,g}_{CO}$. Instead, it introduces an additional parameter K^g_{CS}, which describes the curvature of a wavefront in a common shot gather, evaluated at the receiver position. In conclusion, they present the traveltime expression

$$\begin{aligned} T^2_{FO}(x_m,h) \quad = \quad & \left[T_0 + \left(\frac{\sin\alpha_g}{V_g} - \frac{\sin\alpha_s}{V_s}\right)\Delta x_m + \left(\frac{\sin\alpha_g}{V_g} + \frac{\sin\alpha_s}{V_s}\right)\Delta h\right]^2 \\ & + T_0\left[(4\,K^g_{CS} - 3K^g_{CMP})\frac{\cos^2\alpha_g}{V_g} - K^{\mathrm{s}}_{CMP}\frac{\cos^2\alpha_s}{V_s}\right]\Delta x_m^2 \\ & + T_0\left[K^g_{CMP}\frac{\cos^2\alpha_g}{V_g} - K^{\mathrm{s}}_{CMP}\frac{\cos^2\alpha_s}{V_s}\right]\Delta h^2 \\ & + 2\,T_0\left[K^g_{CMP}\frac{\cos^2\alpha_g}{V_g} + K^{\mathrm{s}}_{CMP}\frac{\cos^2\alpha_s}{V_s}\right]\Delta h\,\Delta x_m \quad . \end{aligned} \tag{14}$$

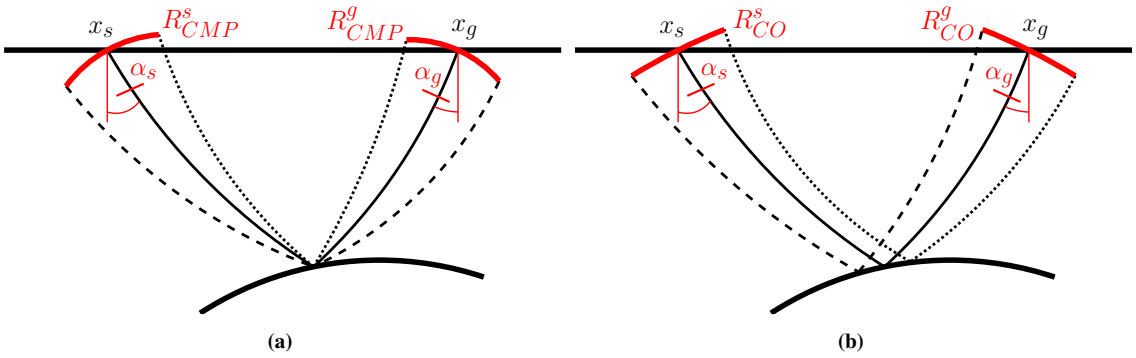

Figure 2: The meaning of the FO-CRS parameters: $K^s_{CMP} = 1/R^s_{CMP}$ ($K^g_{CMP} = 1/R^g_{CMP}$) is the curvature of a wavefront of a CMP experiment, measured at the source (receiver) position; $K^s_{CO} = 1/R^s_{CO}$ ($K^g_{CO} = 1/R^g_{CO}$) is the wavefront curvature of a wavefront of a common offset experiment, measured at the source (receiver); and α_s (α_g) is the emergence (incidence) angle at the source (receiver).

Instead of retaining the unintuitive Δx_m^2 term, however, we suggest a traveltime expression for the FO case that relates more closely to the ZO equation (6) than that by Zhang et al. (2001). Our modified FO traveltime is given by

$$\begin{aligned} T^2_{FO}(x_m, h) \;=\; & \left[T_0 + \left(\frac{\sin\alpha_g}{V_g} - \frac{\sin\alpha_s}{V_s}\right)\Delta x_m + \left(\frac{\sin\alpha_g}{V_g} + \frac{\sin\alpha_s}{V_s}\right)\Delta h\right]^2 \\ & + T_0\left[\frac{\cos^2\alpha_g}{V_g}\,K^g_{CO} - \frac{\cos^2\alpha_s}{V_s}\,K^s_{CO}\right]\Delta x_m^2 \\ & + T_0\left[\frac{\cos^2\alpha_g}{V_g}\,K^g_{CMP} - \frac{\cos^2\alpha_s}{V_s}\,K^s_{CMP}\right]\Delta h^2 \\ & + 2\,T_0\left[\frac{\cos^2\alpha_g}{V_g}\,K^g_{CMP} + \frac{\cos^2\alpha_s}{V_s}\,K^s_{CMP}\right]\Delta x_m\,\Delta h \quad . \end{aligned} \tag{15}$$

As a consequence of equation (13), the mixed term can also be expressed by the $K^{s,g}_{CO}$ because

$$\frac{\cos^2\alpha_g}{V_g}\,K^g_{CMP} + \frac{\cos^2\alpha_s}{V_s}\,K^s_{CMP} = \frac{\cos^2\alpha_g}{V_g}\,K^g_{CO} + \frac{\cos^2\alpha_s}{V_s}\,K^s_{CO} \quad . \tag{16}$$

This follows again from the fact that there are only five independent parameters.

In the ZO case, we find that with $V_g = V_s = V_0$

$$\begin{aligned} \alpha_g = \quad -\alpha_s \quad &= \alpha \quad , \\ K^g_{CMP} = -K^s_{CMP} &= K_{NIP} \quad , \\ K^g_{CO} = \; -K^s_{CO} \quad &= K_N \quad , \end{aligned} \tag{17}$$

and the FO traveltime becomes the ZO traveltime described by equation (9).

Due to the symmetric structure and the more intuitive parametrisation, we suggest to use equation (15) rather than (14). This advantage is particularly useful for the application to predicting FO-CRS attributes, e.g., from known ZO parameters, which we address in the following section.

Prediction of wavefield attributes

Since we need to distinguish between actual, i.e., known, and predicted attributes in this section, we will from now on denote the actual attributes with the subscript 0.

Our approach to predicting FO-CRS parameters from ZO or FO parameters of a neighbouring CMP is inspired by the ray propagator method (e.g., Bortfeld, 1989). Within this concept, the slownesses at sources and receivers at s and g in a paraxial vicinity (e.g., Červený, 2001) of a source and receiver at s_0 and g_0 can be expressed by

$$\begin{aligned} p(s,g) &= p_0 + S_0\,\Delta s + N_0\,\Delta g \quad , \\ q(s,g) &= q_0 + G_0\,\Delta g - N_0\,\Delta s \quad . \end{aligned} \tag{18}$$

This result stems from a first-order derivation with respect to the source and receiver position, respectively, of the underlying parabolic traveltime approximation. It can be applied for the extrapolation of the slownesses, e.g., from zero to finite offset or from one finite offset to another. An according extrapolation for the second-order derivatives, however, fails because further spatial derivation of (18) only leads to $S(s,g) = S_0$, $G(s,g) = G_0$, and $N(s,g) = N_0$.

If, however, we assume a hyperbolic traveltime operator, we can not only derive expressions for the first- but also for the second-order derivatives and apply these to extrapolate the coefficients.

For the derivatives of the hyperbolic traveltime equation in source-receiver coordinates, equation (1), we find (including the traveltime as zero-order derivative),

$$\begin{aligned} T &= \sqrt{(T_0 + q_0\,\Delta g - p_0\,\Delta s)^2 + T_0\,(G_0\,\Delta g^2 - S_0\,\Delta s^2 - 2\,N_0\,\Delta s\,\Delta g)} \quad , \\ q &= \frac{q_0\,(T_0 + q_0\,\Delta g - p_0\,\Delta s) + T_0\,(G_0\,\Delta g - N_0\,\Delta s)}{T} \quad , \\ p &= \frac{p_0\,(T_0 + q_0\,\Delta g - p_0\,\Delta s) + T_0\,(S_0\,\Delta s + N_0\,\Delta g)}{T} \quad , \\ G &= \frac{T_0\,G_0 + q_0^2 - q^2}{T} \quad , \\ S &= \frac{T_0\,S_0 - p_0^2 + p^2}{T} \quad , \\ N &= \frac{T_0\,N_0 + p_0\,q_0 - p\,q}{T} \quad . \end{aligned} \tag{19}$$

In midpoint and half-offset, we find the according expressions for the prediction of the wavefield attributes from one offset and CMP to another offset and CMP:

$$\begin{aligned} \frac{\sin\alpha_g}{V_g} = q &= \frac{T_0}{T}\left[q_0 + \frac{\cos^2\alpha_{g_0}}{V_{g_0}}\,(K^g_{CO_0}\,\Delta x_m + K^g_{CMP_0}\,\Delta h)\right] \\ &\quad + \frac{q_0}{T}\,[(q_0 - p_0)\Delta x_m + (q_0 + p_0)\Delta h] \quad , \\ \frac{\sin\alpha_s}{V_s} = p &= \frac{T_0}{T}\left[p_0 + \frac{\cos^2\alpha_{s_0}}{V_{s_0}}\,(K^s_{CO_0}\,\Delta x_m - K^s_{CMP_0}\,\Delta h)\right] \\ &\quad + \frac{p_0}{T}\,[(q_0 - p_0)\Delta x_m + (q_0 + p_0)\Delta h] \quad . \end{aligned} \tag{20}$$

For simplicity, we keep p and q to express the wavefront curvatures, i.e.,

$$\begin{aligned}
K^g_{CO} &= \frac{V_g}{T\,\cos^2\alpha_g}\left[T_0\,\frac{\cos^2\alpha_{g_0}}{V_{g_0}}\,K^g_{CO_0} + q\,p - q^2 + q_0^2 - q_0\,p_0\right] \quad , \\
K^s_{CO} &= \frac{V_s}{T\,\cos^2\alpha_s}\left[T_0\,\frac{\cos^2\alpha_{s_0}}{V_s}\,K^s_{CO_0} - p\,q + p^2 - p_0^2 + p_0\,q_0\right] \quad , \\
K^g_{CMP} &= \frac{V_g}{T\,\cos^2\alpha_g}\left[T_0\,\frac{\cos^2\alpha_{g_0}}{V_{g_0}}\,K^g_{CMP_0} - q\,p - q^2 + q_0^2 + q_0\,p_0\right] \quad , \\
K^s_{CMP} &= \frac{V_s}{T\,\cos^2\alpha_s}\left[T_0\,\frac{\cos^2\alpha_{s_0}}{V_{s_0}}\,K^s_{CMP_0} + p\,q + p^2 - p_0^2 - p_0\,q_0\right] \quad . \qquad (21)
\end{aligned}$$

In these expressions, the traveltime T is given by equation (15).

For the special case of extrapolation from zero- to finite-offset, these expressions reduce to

$$\begin{aligned}
T &= \sqrt{(T_0 + 2\,q_0\,\Delta x_m)^2 + 2\,T_0\,\frac{\cos^2\alpha}{V_0}\left(K_N\,\Delta x_m^2 + K_{NIP}\,h^2\right)} \quad , \\
\frac{\sin\alpha_g}{V_g} &= q = \frac{T_0}{T}\left[q_0 + \frac{\cos^2\alpha}{V_0}\left(K_N\,\Delta x_m + K_{NIP}\,h\right)\right] + \frac{2\,q_0^2}{T}\,\Delta x_m \quad , \\
\frac{\sin\alpha_s}{V_s} &= p = -\frac{T_0}{T}\left[q_0 + \frac{\cos^2\alpha}{V_0}\left(K_N\,\Delta x_m - K_{NIP}\,h\right)\right] - \frac{2\,q_0^2}{T}\,\Delta x_m \quad . \qquad (22)
\end{aligned}$$

Again, we keep p and q to express the wavefront curvatures, i.e.,

$$\begin{aligned}
K^g_{CO} &= \frac{V_g}{T\,\cos^2\alpha_g}\left[T_0\,\frac{\cos^2\alpha}{V_0}\,K_N + q\,p - q^2 + 2\,q_0^2\right] \quad , \\
K^s_{CO} &= -\frac{V_s}{T\,\cos^2\alpha_s}\left[T_0\,\frac{\cos^2\alpha}{V_0}\,K_N + p\,q - p^2 + 2\,q_0^2\right] \quad , \\
K^g_{CMP} &= \frac{V_g}{T\,\cos^2\alpha_g}\left[T_0\,\frac{\cos^2\alpha}{V_0}\,K_{NIP} - q\,p - q^2\right] \quad , \\
K^s_{CMP} &= -\frac{V_s}{T\,\cos^2\alpha_s}\left[T_0\,\frac{\cos^2\alpha}{V_0}\,K_{NIP} - q\,p - p^2\right] \quad . \qquad (23)
\end{aligned}$$

APPLICATION

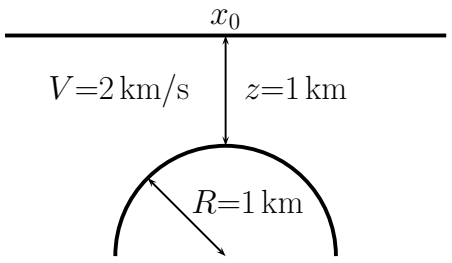

Figure 3: The generic model used in this study.

We have carried out a study with the generic model of a circular reflector in a homogeneous medium for which traveltimes can be calculated analytically (see, e.g., Vanelle, 2013). The reflector and acquisition

geometry are shown in Figure 3. A reflector radius of 1 km was chosen in order to evaluate the feasibility for high reflector curvatures since, as stated above, the extrapolation is exact for planar reflectors.

Traveltimes were generated for midpoints between ± 100 m from x_0 and for offsets up to 1 km. Wavefield attributes were determined by numerical differentiation of the traveltimes according to Vanelle and Gajewski (2002), who have shown that the first- and second-order coefficients can be determined with high accuracy. Since a direct computation of the attributes was not possible for the offset case, we used these values as reference for the comparison with extrapolated results.

We calculated the zero-offset parameters α, R_N, and R_{NIP} analytically and used these as input for the extrapolation from ZO to offsets up to 1 km and midpoint deviations up to $\pm$ 100 m. The considered midpoint range is smaller because whereas the CRS expression is assumed to be accurate for offset/target ratios of approximately one, only few traces around the considered CMP should be taken into account. Therefore, an extrapolation to these distances reaches the limit of the applicability of the CRS formulation.

Figures 4 and 5 show the relative errors of the first-order derivatives, i.e., the horizontal slownesses at the source and receiver and the corresponding incidence and emergence angles, respectively. We recognise that these coefficients were extrapolated with high accuracy within the investigated range.

Of the second-order derivatives in source-receiver coordinates displayed in Figure 6, the coefficients S and G could be determined with higher accuracy than the mixed term N. For the wavefront curvatures, we find in Figure 7 that the accuracy of $K_{CMP}^{S,G}$ is higher than that of $K_{CO}^{S,G}$. This fact reflects that in the ZO CRS, the corresponding parameter K_N is the most unstable one. The reason is that, whereas α is constrained to $\pm 45^\circ$ for most geological situations, and R_{NIP} is positive and of the magnitude of the reflector depth, the radius R_N and thus the curvature K_N can vary between $\pm\infty$. This problem can be accounted for by a projection to the Riemann sphere (Mann, 2002), which we will, however, not elaborate in this paper.

Altogether, we conclude that our method allows the extrapolation from ZO to the offset case with reasonable accuracy even in the presence of the highly-curved reflector considered in our numerical case study.

CONCLUSIONS AND OUTLOOK

We have introduced a new parametrisation for the finite-offset CRS. The resulting traveltime expression is more intuitive than previous parametrisations and permits the prediction of finite-offset parameters from zero offset or another finite offset. Whereas the expressions for the traveltimes as well as for the extrapolated parameters are exact for planar reflectors of arbitrary inclination in a constant velocity background, we have shown with a generic example that the prediction leads to parameters with good accuracy also for curved reflectors.

This work was basically a feasibility study for the suggested method. Since we have now established that the method leads to encouraging results, we will investigate the suitability of the predicted parameters as input for finite-offset CRS stacking. Another important application is to use the predicted FO parameters for partial stacking instead of the currently employed ZO parameters. Since the FO parameters will better fit the data, in particular for higher offsets, we expect that the prestack data enhancement will perform better with these parameters.

ACKNOWLEDGEMENTS

We are grateful to the members of the Applied Seismics Group in Hamburg for continuous and inspiring discussion, in particular to Benjamin Schwarz and Jan Walda. This work was partially supported by the sponsors of the Wave Inversion Technology (WIT) consortium.

REFERENCES

Bauer, A., Schwarz, B., and Gajewski, D. (2014a). From ZO to CO with diffractions: complex data examples. *Annual WIT report*, 18.

Bauer, A., Schwarz, B., and Gajewski, D. (2014b). From ZO to CO with diffractions: theory. *Annual WIT report*, 18.

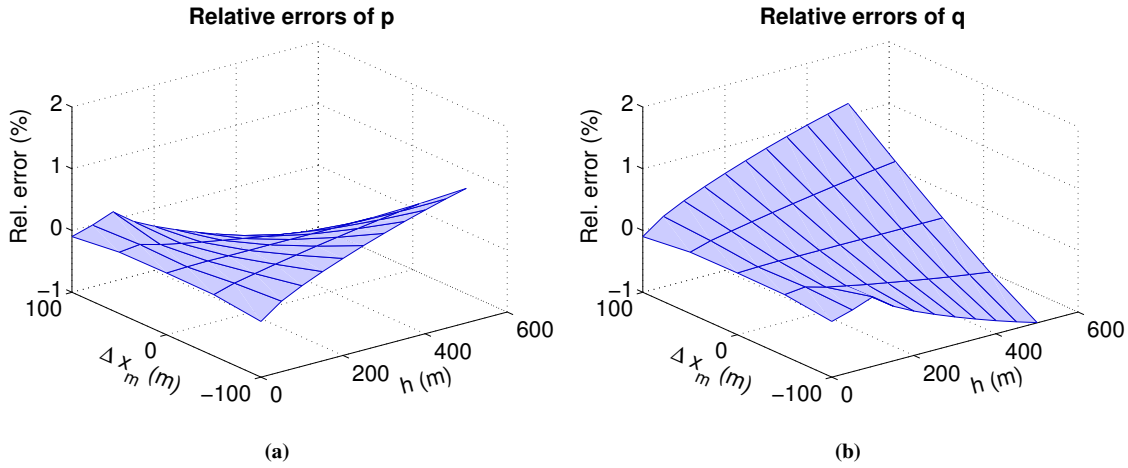

Figure 4: Relative errors of the extrapolated first-order derivatives in source-receiver notation: horizontal slownesses (a) at the source and (b) at the receiver.

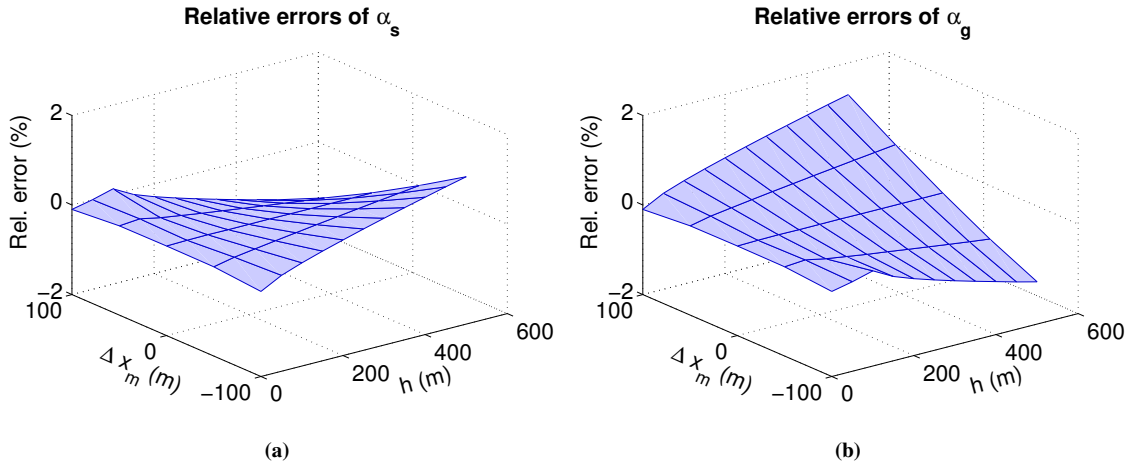

Figure 5: Relative errors of the extrapolated angles in source-receiver notation: (a) at the source and (b) at the receiver.

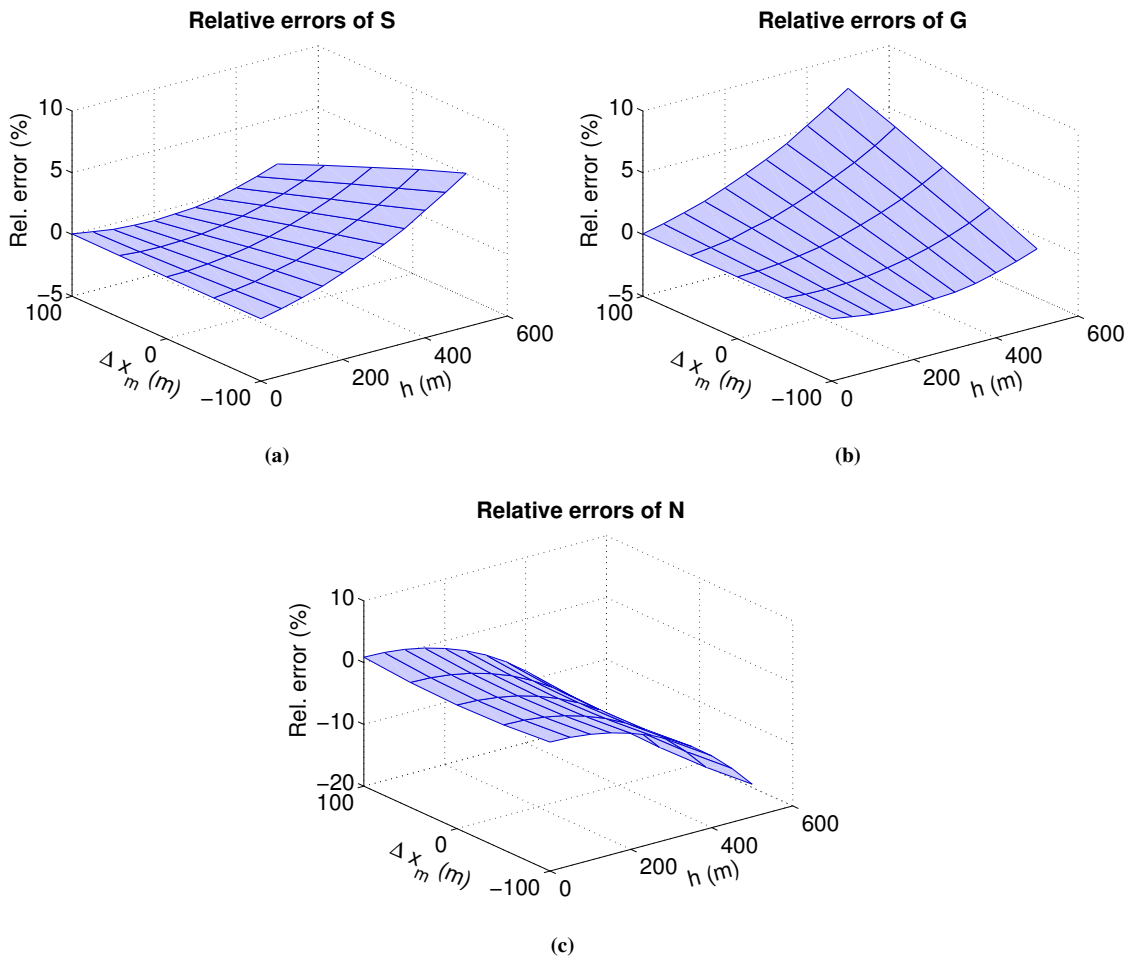

Figure 6: Relative errors of the extrapolated second-order derivatives in source-receiver notation: (a) with respect to the source, (b) the receiver, (c) the mixed derivative.

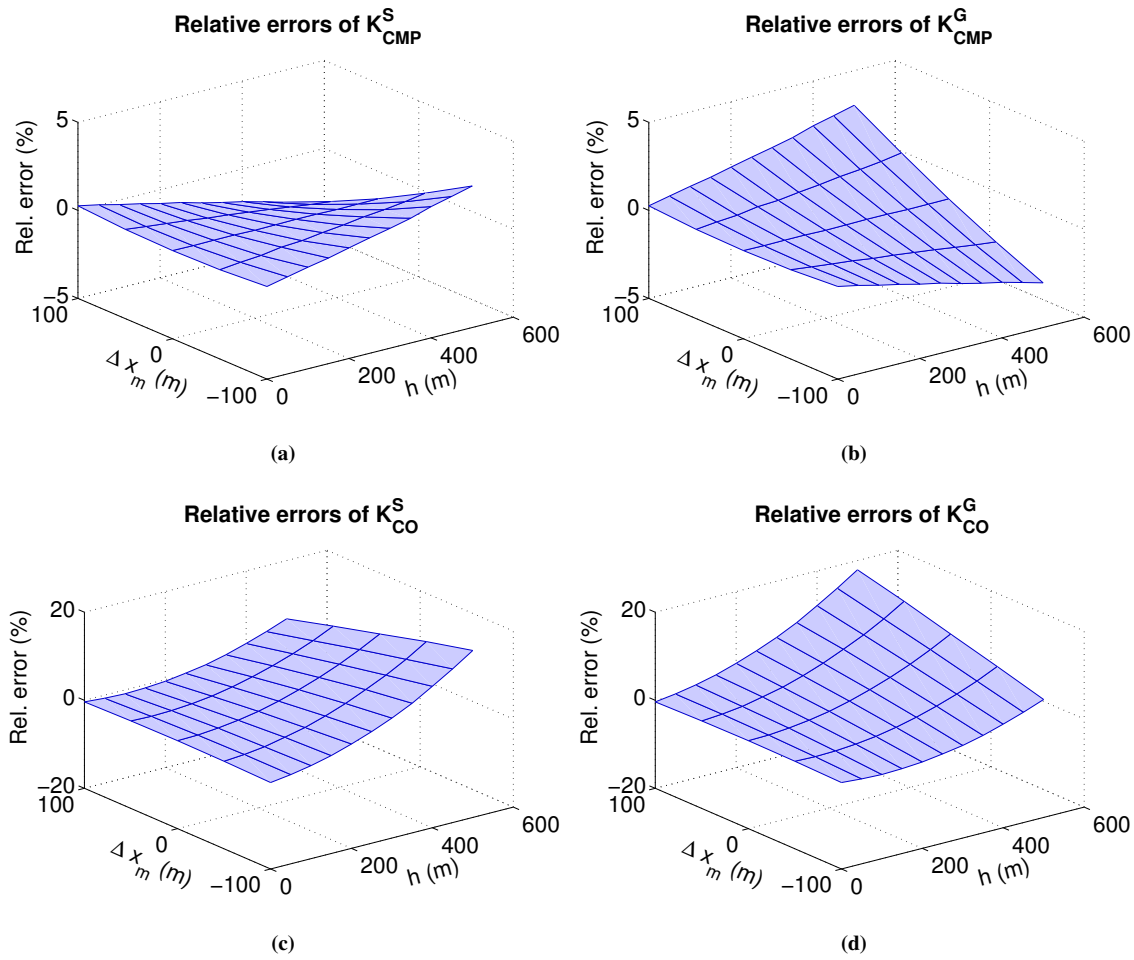

Figure 7: Relative errors of the extrapolated wavefront curvatures.

Baykulov, M. and Gajewski, D. (2009). Prestack seismic data enhancement with partial Common Reflection Surface (CRS) stack. *Geophysics*, 74:V49–V58.

Bortfeld, R. (1989). Geometrical ray theory: rays and traveltimes in seismic systems (second-order approximations of the traveltimes). *Geophysics*, 54:342–349.

Červený, V. (2001). *Seismic Ray Theory*. Cambridge University Press.

de Bazelaire, E. (1988). Normal moveout revisited – inhomogeneous media and curved interfaces. *Geophysics*, 53:143–157.

Gelchinksy, B., Berkovitch, A., and Keydar, S. (1999). Multifocusing homeomorphic imaging – Part 1. Basic concepts and formulae. *Journal of Applied Geophysics*, 42:229–242.

Jäger, R., Mann, J., Höcht, G., and Hubral, P. (2001). Common-reflection-surface stack: Image and attributes. *Geophysics*, 66:97–109.

Landa, E., Keydar, S., and Moser, T. J. (2010). Multifocusing revisited – inhomogeneous media and curved interfaces. *Geophysical Prospecting*, 58:925–938.

Mann, J. (2002). *Extensions and applications of the Common-Reflection-Surface Stack method*. PhD thesis, University of Karlsruhe.

Müller, T. (1999). *The Common Reflection Surface stack method – seismic imaging without explicit knowledge of the velocity model*. PhD thesis, University of Karlsruhe.

Schwarz, B., Vanelle, C., Gajewski, D., and Kashtan, B. (2014). Curvatures and inhomogeneities: an improved common-reflection-surface approach. *Geophysics*, 79:S231–S240.

Vanelle, C. (2012). *Stacking and migration in an/isotropic media*. Habilitation thesis, University of Hamburg.

Vanelle, C. (2013). Reflections from a spherical interface. *Annual WIT report*, 17:254–277.

Vanelle, C. and Gajewski, D. (2002). Second-order interpolation of traveltimes. *Geophysical Prospecting*, 50:73–83.

Vanelle, C., Kashtan, B., Dell, S., and Gajewski, D. (2010). A new stacking operator for curved subsurface structures. *Annual WIT report*, 14:247–254.

Zhang, Y., Bergler, S., , and Hubral, P. (2001). Common-reflection-surface (CRS) stack for common offset. *Geophysical Prospecting*, 49:709–718.

Zhang, Y., Bergler, S., Tygel, M., and Hubral, P. (2002). Model-independent traveltime attributes for 2D finite-offset multicoverage reflections. *Pure and Applied Geophysics*, 159:1601–1616.